Acta Crystallographica Section A
Foundations of Crystallography
ISSN 0108-7673

Received 16 February 2011
Accepted 25 March 2011

Anomalous extinction of X-rays diffracted in strongly deformed crystals

Michael Shevchenko

Institute for Metal Physics, 36 Vernadsky Street, Kiev 03142, Ukraine. Correspondence e-mail: mishevch@yahoo.com

The extinction concept is extended for very thin non-ideal crystals. It is shown that for a large gradient, the integrated reflected intensity exhibits a prominent extinction minimum. This anomaly is an interbranch effect, occurring for crystals with thicknesses of the order of the interbranch extinction length. Different possibilities for applying this newly developed extinction theory to X-ray integrated wave topography are discussed.

1. Introduction

As is well known, the dynamical interchange of the energy of X-rays diffracted in a thick perfect crystal may lead to a decrease in intensity of the primary beam. In the transmitted diffraction this effect, called the primary extinction, is associated with the divergence problem of integrated reflected intensities. This problem is completely removed due to extinction of the incident radiation (Authier, 2005). However, the primary extinction effect will disappear for X-rays scattered by a strongly deformed region, where the effective misorientation exceeds the perfect crystal range $\Delta\psi_{\rm D}$.

In this paper we will present the theory of a new extinction phenomena, which we will refer to as anomalous extinction. This phenomenon also occurs in transmission geometry when the crystal thickness is considerably less than the X-ray extinction length ξ_g for an ideal crystal. It should be noted that the new X-ray diffraction methods used to study materials in small dimensions (such as coherent diffraction, microdiffraction, X-ray diffraction line-profile modeling *etc.*) show that such small crystals may be found in states of very high stress (Robinson & Vartanyants, 2001; Tanuma *et al.*, 2007; Scardi, 2004). In this connection it is assumed that the crystals are also strongly deformed. For strong lattice distortions we will assume that the strain field is specified by the strain gradient, which is considerably greater than $1/\xi_g^2$. This condition is equivalent to the deformation of the lattice over the unit distance being much greater than a rotation of the order of the width of the rocking curve over a distance equal to the *Pendellösung* distance ξ_g. Moreover, when this condition is satisfied the eikonal approximation of the dynamical theory is no longer valid (Authier & Balibar, 1970). At the same time, despite the large value of the strain gradient, the displacement $\mathbf{u}$ may be small in comparison to the lattice spacing.

It is worth noting that in strongly deformed crystals the redistribution of energy between transmitted and diffracted waves may be considerably affected by interbranch scattering. As was shown by Shevchenko (2007), the prominent features seen in the X-ray rocking curve from highly distorted crystals are due to interbranch scattering. It is natural to suggest that these peculiarities are related to the appreciable extinction of X-rays. This point and the mechanism of anomalous extinction will be considered in detail in the next section. Moreover, we will also discuss the application of the extinction effect to X-ray integrated wave topography.

2. Results

Takagi's equations are commonly used to describe X-ray dynamical diffraction in deformed crystals when long-range strain fields are distributed in the crystal. For any form of displacement $\mathbf{u}$, they can only be analytically solved for a weak deformation (Penning & Polder, 1961; Kato, 1963). This solution specifies X-ray into-a-branch scattering and corresponds to the eikonal approximation of dynamical theory. With a constant strain gradient, the analytical solution of Takagi's equations can be expressed in terms of confluent hypergeometric functions (Litzman & Janacek, 1974; Chukhovski, 1974; Katagawa & Kato, 1974). However, an asymptote of this solution for strong lattice distortions does not describe the X-ray multiple scattering, which occurs in a small vicinity $\Delta z_{\rm D}$ of the point z_0, where the Bragg condition is locally satisfied (Shevchenko, 2009). Thus, the point z_0 is characteristic of the solution of the diffraction problem. It can be considered to be the real part of the complex turning point (Chukhovski, 1980). To find a solution near the turning point it is necessary to rearrange a given equation to one which would only describe the interchange of the eikonal modes. Unfortunately, due to the complexity of the turning point, the standard method of rearrangement of the differential equations (as described, for example, in Nayfeh, 1993) is not applicable to the X-ray diffraction problem. With this in mind, an original approach, which is similar to the Lagrange method, was developed (Shevchenko, 2005). Assuming a one-dimensional displacement $\mathbf{u}(z)$, which depends on the depth z in the crystal, Takagi's equations were reduced to a set of differential equations describing the interbranch contribution

near the point z_0. For the transmitted wave, these equations have the form

$$\frac{\mathrm{d}A_0^{1,2}(z)}{\mathrm{d}z} = -\frac{A_0^{2,1}(z)\exp\{\mp 2iz\pi/\xi_g\}\int_0^z p(z_i)\,\mathrm{d}z_i}{2p^2(z)[\omega \pm (1+\omega^2)^{1/2}]}\frac{\mathrm{d}\eta(z)}{\mathrm{d}z}. \quad (1)$$

Here $p(z) = [1+\eta^2(z)]^{1/2}$, where $\eta(z) = \omega + (\mathbf{g}\,\mathrm{d}\mathbf{u}(z)/\mathrm{d}z) \times \xi_g/(2\pi)$, $\omega = s\xi_g/(2\pi)$ and s is the deviation of the incident wave from Bragg's law. The values $A_0^{1,2}(z)$ are amplitudes of the transmitted waves within the eikonal representation, which correspond to the different branches of the local dispersion surface. They are related to the amplitude of the plane-wave expansion $D_0(z)$ by

$$D_0(z) = \exp\left\{i\int_0^z q(z_1)\,\mathrm{d}z_1\right\}\sum_{j=1,2} A_0^j(z)\phi_0^j(z), \quad (2)$$

where $\phi_0^{1,2}(z)$ are the 'eikonal solutions' for the transmitted wave of Takagi's equation. Thus, equation (2) introduces the 'eikonal representation' of dynamical theory, which only describes X-ray interbranch scattering. Equations (1) and (2) are expressed more fully in Shevchenko (2009, §2), where the analytical expressions of the eikonal solutions are also given.

Clearly, solving equation (1) is a difficult problem. However, equation (1) can be solved approximately for homogeneous bending (Shevchenko, 2007). From this result, the amplitudes $D_{0,g}$ of the transmitted and diffracted waves can be written in the form

$$D_0(z) = \exp\left\{i\int_0^z [q(z_1) + \theta(z_0 - z_1)Q(z_1)]\,\mathrm{d}z_1\right\}, \quad (3)$$

$$D_g(z) = \frac{i\pi}{\xi_g}\int_0^z \exp\{i[-\omega\pi/\xi_g + \theta(z_0 - z_1)Q(z_1)]z_1\}\,\mathrm{d}z_1, \quad (4)$$

where $q(z) = [s + \mathbf{g}\,\mathrm{d}\mathbf{u}(z)/\mathrm{d}z]/2$ and $Q(z) = \pi[(p(z)/\xi_g)^2 + (\Lambda_0 p(z))^{-2}]^{1/2}$. Here $\Lambda_0 = 2\xi_g/\varepsilon$ is the X-ray interbranch length, where $\varepsilon = \alpha g\xi_g^2/(2\pi^2 R)$. It is also assumed that the displacement $u(z) = \alpha z^2/(2R)$, where α and R are constants describing the deformation and the radius of curvature, respectively. The interbranch jump of the tie point is taken into account using the step function $\theta(z_0 - z)$, which equals 1 and -1 if $z_0 - z > 0$ and $z_0 - z < 0$, respectively. As seen from equation (3), in strongly bent crystals multiple scattering only contributes to the $D_0(z)$ phase, while the amplitude changes caused by this process are disregarded due to being negligible. It should be noted that in equation (4) the interbranch contribution to $D_g(z)$ is integrated over the crystal thickness. Nevertheless, interbranch scattering is able to produce the prominent features of the diffracted intensity even after integrating over the crystal thickness.

It is necessary to point out that equations (3) and (4) are obtained using the assumption that any attenuation of the incident wave by diffraction through the crystal is neglected. In fact, this means that all the energy of the incident wave is transferred from the upper dispersion branch to the lower dispersion branch, with z_0 at one point. Meanwhile, the interbranch redistribution of the energy will occur within a certain vicinity of the point z_0. Clearly this correction is not critical for the prediction of phase modulation effects for the diffracted intensity because they are caused by sharp changes in the phase of the X-ray wavefields, originated in the interbranch jump of the tie point. However, due to an accumulation of systematic errors, this correction may be important for the calculation of the integrated reflected intensity. With this in mind we modified the expression for the amplitude $D_g(z)$ as follows, assuming for simplicity that the vector diffraction $\mathbf{g}$ is parallel to the displacement $\mathbf{u}$.

$$\begin{aligned} D_g(z) = {} & \frac{i\pi}{\xi_g}\int_0^z \exp\{-2i\omega z_1\pi/\xi_g + igu(z_1)\}\,\mathrm{d}z_1 \\ & + \frac{i\pi}{\xi_g}\exp\{-|z - z_0|/\Lambda_0\} \\ & \times \left\{\int_0^z \exp\big\{i\big[-\omega\pi/\xi_g + \theta(z_0 - z_1)Q(z_1)\big]z_1\big\}\,\mathrm{d}z_1\right. \\ & \left. - \int_0^z \exp\{-2i\omega z_1\pi/\xi_g + igu(z_1)\}\,\mathrm{d}z_1\right\}. \end{aligned} \quad (5)$$

In equation (5) we separate the contributions from different processes. The first term only corresponds to the kinematical diffraction, whereas the second term in equation (5) only specifies the multiple scattering contribution. Since the multiple scattering is responsible for the spatial distribution of the energy in the vicinity of point z_0, the second term is multiplied by the factor $\exp\{-|z - z_0|/\Lambda_0\}$. In doing so, we take into consideration empirically that redistribution of the energy is effective within the range Δz_D, of the order of the X-ray interbranch extinction length Λ_0, specifying the range of the dynamical diffraction in strongly bent crystals. It also follows from this that the interbranch contribution to the X-ray wavefields is appreciable within the vicinity of Δz_D. Beyond this vicinity, due to the exponential factor, the amplitude of the diffracted wave will rapidly tend towards the kinematical limit.

Equation (5), as well as equation (4), describes the interbranch 'fine' structure effects which occur for crystals with thicknesses of $t \simeq \Lambda_0$. Considering the amplitude D_g as a function of the deviation ω results in splitting of the diffracted intensity $I_g(\omega)$, plotted in Figs. 1(*a*) and (*b*). These curves, calculated using equation (5), correspond to (*a*) a deformation $\varepsilon = 100$ and a thickness $T = 1$ (in units of t/Λ_0) and (*b*) a deformation $\varepsilon = 200$ and a thickness $T = 2$. These model parameters can be applied to the conventional case of X-ray diffraction, specified by the values $\xi_g = 10^{-5}$ m, $g = 2\pi \times 10^{10}$ m^{-1}. In this case, the thickness t corresponding to the model parameters is 200 nm, such that the X-ray interbranch extinction length Λ_0 = 200 and 100 nm for deformations ε = 100 and 200, respectively. Moreover, one can estimate that the appropriate radius of curvature R is of the order of 10^{-2} m and, consequently, the displacement u does not exceed a few %. Thus, displacement u is a small value,

while the strain gradient proportional to the value g/R is considerably greater than $1/\xi_g^2$.

It can be established by analyzing the splitting of Bragg's peak that the diffracted intensity increases by varying the deviation ω from $\omega_M = -2\pi t/\Lambda_0$ to 0, such that it is minimal when $\omega = \omega_M$ and maximal when $\omega = 0$. [Indeed, when $\omega = \omega_M$, the period of oscillations of the integrands in equations (4) and (5) is less than for $\omega = 0$. Then from equations (4) and (5) it can be deduced that the diffracted intensity has a minimum at ω_M and a maximum at $\omega = 0$ by integrating over z]. It should be noted that, due to the complementary of the diffracted and transmitted intensities, the transmitted intensity will decrease when the deviation varies from ω_M to 0. Obviously, this effect can be considered as an extinction of X-rays, which occurs in the case of X-ray diffraction by a strongly deformed crystal.

Since the interval of variation of the deviation ω, corresponding to the extinction effect, coincides with the range of activation of the interbranch scattering, it is known as the interbranch effect. Clearly such an effect will be most prominent for the diffracted intensity. In this case, the significant extinction changes of the diffracted intensity are due to the interbranch phase modulation of the X-ray wavefields. The period of modulation may be estimated as Λ_0, which is of the order of the crystal thickness. Therefore, the integration of the interbranch contribution over the crystal thickness leads to pronounced splitting of Bragg's peak, which is accompanied by an increase in the diffracted intensity within the deviation interval from ω_M to 0.

The specific character of X-ray extinction in strongly deformed crystals will be referred to as anomalous extinction. We also refer to anomalous notation as being the extinction property caused by strong lattice distortions. This property is actually an unusual feature of X-ray extinction. Strong deformations are well known to suppress the primary and secondary extinction effects. On the other hand, the anomalous extinction increases with strengthening deformation. Indeed, considering the position of the extinction minimum in Figs. 1(*a*) and (*b*), the range of activation of this effect can be seen to increase with increasing deformation. An increasing gradient leads to an appropriate increase in the value of ω_M. For example, for ε = 200 this value doubles compared with the value corresponding to ε = 100.

Thus we can deduce that the mechanism of extinction of X-rays is determined mainly by the degree of perfection of the crystal. In an ideal or a slightly deformed crystal the X-ray extinction is caused by into-the-branch scattering, which produces the amplitude modulation of the X-ray wavefields. On the other hand, in a highly deformed crystal X-ray extinction is due to interbranch scattering, which produces the phase modulation of the X-ray wavefields. It is important to note that the anomalous extinction effect turns out to be prominent in the integrated reflected intensity. By numerically integrating equation (5) over the deviation ω, the integrated intensity was calculated for model deformation $\varepsilon = 100$ and $\varepsilon = 200$. Moreover, for convenience we introduce the normalized intensity $I_g^{\rm int}$ as the ratio of the integrated reflected intensity and the kinematical intensity. Obviously, the normalized intensity $I_g^{\rm int}$ can also be considered as the correction for anomalous extinction. Figs. 2(*a*) and (*b*) show plots *versus* crystal thickness T (in units t/Λ_0). The intensity shows the pronounced extinction minimum which corresponds to a crystal thickness of the order of the interbranch extinction length Λ_0. With increasing thickness, the intensity tends towards the kinematical limit, exhibiting more-or-less periodic oscillations. Their period approximately corresponds to a thickness change of the order of Λ_0. They originate in the interbranch oscillations of the diffracted intensity as a function of crystal thickness, as described in Shevchenko (2007).

It should also be noted that the semi-empirical character of equation (5) does not influence the appearance of the extinction minimum in the integrated diffracted intensity. In fact, this minimum is due to the interbranch splitting of the X-ray rocking curve. In equations (4) and (5) the splitting effect is described by the term specifying the interbranch jump of the tie point. This term is calculated analytically by summing up the phase of the multiply scattered waves in the bent crystal. On the other hand, the exponential factor,

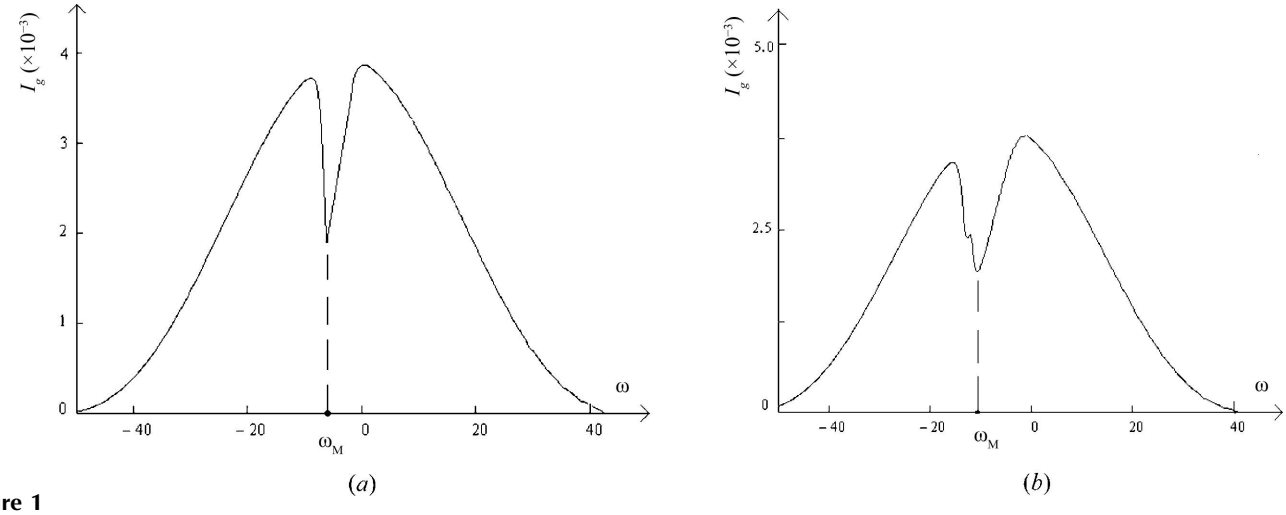

Figure 1
The X-ray rocking curves for the deformations (*a*) $\varepsilon = 100$ and (*b*) $\varepsilon = 200$, such that $\omega_M = -2\pi$ and -4π, respectively.

introduced empirically in equation (5), determines the steepness of the tendency of the integrated intensity to the kinematical limit. Owing to this factor, the intensity will rapidly tend to the limit with increasing thickness of the crystal.

As can be seen in Figs. 2(*a*) and (*b*), the intensity of the extinction minimum increases with an increase in the gradient. For deformation $\varepsilon = 100$, the minimal value of the intensity is approximately 0.86, whereas it is 0.9 for $\varepsilon = 200$. This fact is specific to the normalized integrated intensity. It is due to the broadening and eroding of Bragg's peak caused by the lattice distortion. The integrated intensity, which is the area lying beneath the X-ray rocking curve, increases with increasing deformation. Furthermore, the relation of the square of this area to that of the area of the interbranch losses may increase in this case. As a result, the normalized integrated intensity also increases.

It can be seen that the correction for anomalous extinction has an appreciable value. As follows from the results presented, the anomalous extinction is of the order of 10% in relation to the kinematical limit. At the same time, the correction for primary extinction, given in James (1948), Chapter VI, p. 272, is of the order of 0.01–0.1% for the model parameters $\xi_g \simeq 10^{-5}$ m, $g \simeq 10^{10}\,\mathrm{m}^{-1}$ and $t = 10^{-7}$ m. An increase in the extinction correction by two or three orders of magnitude allows us to use the anomalous extinction effect in X-ray studies of very thin crystals. Obviously, applying the methods of high-resolution X-ray diffraction would be preferable.

3. Discussion

It is clear from Figs. 2(*a*) and (*b*) that the X-ray integrated wave topography is one of the most likely uses of the anomalous extinction phenomenon. Indeed, the non-linear dependence of the integrated intensity *versus* crystal thickness, attributed to the pronounced extinction minimum, implies an appreciable extinction contrast from defects in very thin and strongly deformed crystals. It should be remembered that from the viewpoint of the ordinary extinction effect the lower limit for the thickness of the crystals for defects to give clear contrast in X-ray topographs has been estimated as 1/3 to 1/6 of the *Pendellösung* length (Penning & Goemans, 1968). A more accurate criterion was obtained in Tanner (1972). It follows from this criterion that in low-order reflections the minimum thickness at which good contrast is observed is about $0.4\xi_g$. This value falls to $\sim 0.15\xi_g$ for higher-order reflections.

Following on from the considerations presented, the minimum thickness for the formulation of the anomalous extinction contrast image is of the order of the interbranch extinction length Λ_0. It should be noted that the value of Λ_0 is considerably less than the minimum thickness for visibility of defects as predicted by conventional theory. However, to increase the appreciable width of the defect image it is necessary to suggest that the value of ξ_g is sufficiently large. Bearing this in mind we pay attention to protein crystals, where ξ_g may reach a magnitude 10^{-3} m. Thus, these crystals can also be considered to be a 'magnified' model to test the fundamentals of a given theory. Relating to this it is worth mentioning the paper by Shevchenko (2009), which deals with the X-ray study of the anomalous decrease of the dislocation image in protein crystals. This fact was reported in the work by Koizumi *et al.* (2005), in which the image width of the screw dislocation related to the conventional theory (Authier, 1967) was greater than that measured by two orders of magnitude. Clearly, such a considerable effect cannot be interpreted as a compression of the direct dislocation image caused by the orientation contrast contribution. [This effect was described in Dudley (1999), and implies the compression of the width of the image several times, *i.e.* by less than one order of magnitude.] At the same time the anomalous width of the dislocation image can be easily explained by considering the

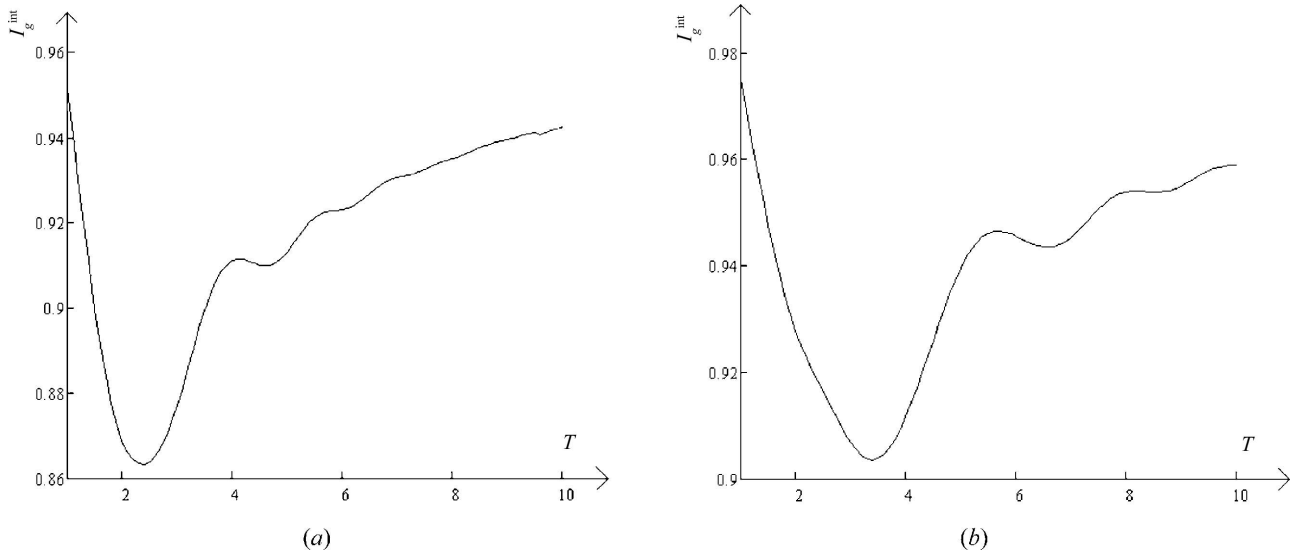

Figure 2
The normalized integrated intensity for (*a*) $\varepsilon = 100$ and (*b*) $\varepsilon = 200$ *versus* crystal thickness T (units t/Λ_0).

interbranch scattering in a small crystal matrix (mosaic block) which is assumed to be strongly deformed. Since the anomalous extinction is the interbranch scattering effect, which is specified by the nonlinear dependence of the integrated intensity *versus* thickness, it can be suggested that this phenomenon is mainly responsible for the anomalous image width in protein crystals.

Besides protein crystals, another example of a possible use of the anomalous extinction effect is the X-ray topography of crystals using quasi-forbidden reflections. These studies are also characterized by a large extinction length ξ_g that makes it practically impossible to obtain direct images of defects in crystals of a reasonable thickness. However, we can predict the observation of such images for deformed crystals by taking into account the X-ray anomalous extinction. In the case of strong and extended lattice distortions, anomalous extinction may lead to the formation of the direct image even for a crystal thickness which is considerably less than the conventional extinction length ξ_g. It should be noted that the problem of observing direct images for diamond crystals of different perfection using forbidden reflections was considered in Shyryaev *et al.* (2008). It was found that the X-ray contrast appears due to the presence of platelet-type defects, such that the topographs show individual dislocations. Analyzing these results, it is relevant to note that the long-range strain fields may be caused by impurities in the crystals. This conclusion was made in the work by Ikeno *et al.* (1968) devoted to the X-ray topographical studies of NaCl crystals grown from an aqueous solution containing Mn ions. With this in mind, we can suggest that the X-ray contrast from the diamond crystal may be due to the anomalous extinction of X-rays. In this case, the strong deformations can be caused by platelet impurities.

Thus, the problem of X-ray extinction contrast is worthy of attention even in the case of a crystal thickness which is considerably less than the conventional length ξ_g. When the crystal is highly deformed the extinction contrast is formed due to X-ray interbranch scattering, which leads to the prominent extinction minimum in the X-ray integrated reflected intensity.

References

Authier, A. (1967). *Adv. X-ray Anal.* **10**, 9–31.
Authier, A. (2005). *Dynamical Theory of X-ray Diffraction*. Oxford University Press.
Authier, A. & Balibar, F. (1970). *Acta Cryst.* A**26**, 647–654.
Chukhovski, F. (1974). *Kristallografiya*, **19**, 482–488.
Chukhovski, F. (1980). *Metallofizika*, **2**, 3–27.
Dudley, M. (1999). *J. Phys. D Appl. Phys.* **32**, A139–A144.
Ikeno, S., Marnyama, H. & Kato, N. (1968). *J. Cryst. Growth*, **3**, 683–693.
James, R. (1948). *The Optcal Principles of the Diffraction of X-rays*. London: G. Bell and Sons.
Katagawa, T. & Kato, N. (1974). *Acta Cryst.* A**30**, 830–836.
Kato, N. (1963). *J. Phys. Soc. Jpn*, **18**, 1785–1791.
Koizumi, H., Tachibana, M., Yoshizaki, I. & Kojima, K. (2005). *Philos. Mag.* **85**, 3709–3713.
Litzman, O. & Janacek, Z. (1974). *Phys. Status Solidi A*, **25**, 663–666.
Nayfeh, A. H. (1993). *Introduction to Perturbation Techniques*. Wiley Classics Library Ed. New York: Wiley-VCH.
Penning, P. & Goemans, A. (1968). *Philos. Mag.* **18**, 297–300.
Penning, P. & Polder, D. (1961). *Philips Res. Rep.* **16**, 419–440.
Robinson, I. & Vartanyants, I. (2001). *Appl. Surf. Sci.* **182**, 186–191.
Scardi, P. (2004). *Proceedings of the XIX Conference on Applied Crystallography*, edited by H. Morawice & D. Stoz, pp. 16–22. Singapore: World Scientific.
Shevchenko, M. (2005). *Acta Cryst.* A**61**, 512–515.
Shevchenko, M. (2007). *Acta Cryst.* A**63**, 273–277.
Shevchenko, M. (2009). *Acta Cryst.* A**65**, 352–359.
Shyryaev, A., Mukhamedzanov, E., Voloshin, A., Morkovin, A., Borisov, M. & Titkov, S. (2008). *JETP Lett.* **88**, 670–673.
Tanner, B. (1972). *Phys. Status Solidi A*, **10**, 381–386.
Tanuma, R., Kuto, T., Togoh, F., Tawura, T., Saito, A., Fukuda, K., Hayashi, K. & Tsusaka, Y. (2007). *Phys. Status Solidi A*, **204**, 2706–2713.